Structures 48 (2023) 147–158

Contents lists available at ScienceDirect

Structures

journal homepage: www.elsevier.com/locate/structures

The effect of joint stiffness on optimization design strategies for gridshells: The role of rigid, semi-rigid and hinged joints

Valentina Tomei

Department of Civil and Mechanical Engineering, University of Cassino and Southern Lazio, Via G. Di Biasio 43, 03043 Cassino, Italy

ARTICLE INFO

Keywords:
Gridshells
Structural optimization
Semi-rigid joints
Global buckling
Imperfections
Steel structures

ABSTRACT

Structural optimization techniques are becoming popular and effective approaches for the design of constructions, able to support architects and structural designers in the complex process of searching competitive solutions, usually in terms of structural weight, cost and accounting for specific structural/functional requirements. In case of gridshells, the structural weight is strictly related to the susceptibility of the structure to global buckling, which is often the governing design criterion. The susceptibility to global buckling is mainly due to the global stiffness of the structures, primarily related to the stiffness of the joints, to the boundary conditions, and to the presence of imperfections. In this context, the paper presents design strategies based on optimization techniques that specifically take into accounts the presence of semi-rigid, rigid and hinged joints in order to guarantee light solutions safe from global buckling phenomena. In particular, two approaches are proposed: the joint stiffness approach, which considers the gridshell composed by semi-rigid joints, all characterized by the same rotational stiffness, and the rigid/hinged approach, which considers the gridshell composed by most hinged joints, and by a low number of rigid joints arranged in optimal positions. The approaches have been applied to a case study characterized by different boundary conditions, different rise-to-span ratios and also considering both perfect and imperfect shapes. The results of the proposed optimization processes highlight the beneficial effect of a finite value of the rotational stiffness of the joints in the susceptibility of the gridshell to global buckling phenomena, leading to light structural solutions.

1. Introduction

In the last two decades, gridshell structures are often adopted in large span systems thanks to their peculiarity to combine aesthetic qualities and optimal structural performances, which are completely merged since the shape is itself the structure. Design strategies based on optimization techniques, currently spreading in the world of both practitioners [1–6] and researchers [7–15], are always more often applied also to gridshell structures because of their capacity to deal with the complex process of searching competitive solutions in terms of structural weight, cost and structural/ functional requirements [16–26].

Gridshell structures are particularly susceptible to global buckling, which mostly represents the predominant design criterion. In this framework, an important role is played by the boundary conditions and the stiffness of the joints, as highlighted by some research works. About the first aspect, the works by Venuti et al. [27,28] analysed the effect of boundary conditions – stiffened or non-stiffened free edges – on the buckling load of the whole gridshell. About the stiffness of the joints, some authors [29–34] consider that the joints can be not only hinged or rigid but also semi-rigid, and their stiffness play a key role in the global stability of the gridshell. In this context, it becomes fundamental to characterize the stiffness of the joints to be used in gridshells and, indeed, recent works carried out experimental and/or numerical investigations to derive the stiffness and the strength of different kind of joints. In particular, Zhang and Feng [35] analysed, from both numerical and experimental points of view, the cyclic behaviour of double-ring joints for gridshells, in order to define their stiffness, bearing capacity and energy dissipation; Han et al. [36,37] derived, from a numerical point of view, the stiffness and the bearing capacity of innovative Assembled Hub joints, and they analysed the effect of the stiffness on the stability of single layer gridshells. Fan et al. [38] performed an experimental campaign in order to define moment-rotation curves of semi-rigid joints, by varying different geometrical parameters. More in details, they analysed socket and bolt-ball joints, generally employed for spatial structures; these joints are both composed by a central ball node, connected to the members through high strength bolts, sleeves and dowel pins, which is a hollow ball in the case of socket joints and a solid ball node in the case of bolt-ball joints. Ma et al. [39] investigated, from both experimental and numerical points of view, a new semi-rigid bolt-column joint constituted by a ring to which H, I and rectangular section members are connected through side plates and pretensioned bolts. Parametric analyses have been performed on the new joint system by

https://doi.org/10.1016/j.istruc.2022.12.096
Received 20 September 2022; Received in revised form 22 December 2022; Accepted 22 December 2022

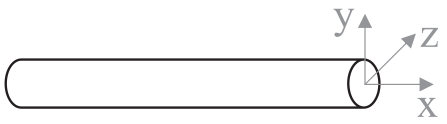

Fig. 1. Local axis of structural members.

varying the thickness of the side plates, the pretension value in the bolts and the bolt diameter. The results highlighted how the different parameters affect the initial stiffness, the flexural resistance and the plastic moment resistance; in particular, the initial stiffness is mainly influenced by the thickness of the side plates and the bolt diameters. Gidófalvy et al. [40] numerically investigated the characteristics in terms of initial stiffness and flexural resistance of a novel joint connecting *T*-cross sections, by varying their dimensions and pretension on the bolts; then, they analysed the effect of these joints on the ultimate bearing capacity of a free-form gridshell with a quadrangular plan. Tsadvaridis et al. [41] proposed a process of shape optimization that specifically takes into account the stiffness of the joints; the process is applied on a series of triangulated gridshells in order to minimize the strain energy: the optimization is carried out by considering different levels of stiffness evaluated on tests performed on semi-rigid ring joints characterized by different geometrical characteristics, which also determine the stiffness of the joints. The results highlight a great influence of the joint stiffness on the results of the shape optimization, in terms of both optimal shape and buckling factor. Recently, the attention has been also focused on aluminium gridshells: in particular, Liu et al. [42] investigated the effect of semi-rigid aluminium joints on the stability of aluminium gridshells, together with the beneficial effect of a stressed skin; on the other hand, Yang et al. [43] carried out an experimental campaign to derive moment-rotational curves of aluminium joints to be employed in gridshell structures, in order to characterize their stiffness and strength by varying the properties of materials and components; Formisano et al. [17,18] investigated the role of joints in the case of aluminum structures, proposing an ad hoc design strategy of nodes and bars for a double-layer reticular space structures [17] and they analysed the nonlinear behaviour of bolted aluminium alloy *T*-stub joints by means of experimental tests and numerical simulations [18].

Downstream of this discussion, the aim of the paper is to propose optimization design strategies for gridshells that specifically take into account the stiffness of the joints, in order to obtain light solutions safe from global buckling phenomena, and including the effect of imperfections. In particular, two optimization strategies are proposed and compared:

- the joint stiffness approach where the gridshell structure is composed by semi-rigid joints, all characterized by the same optimal rotational stiffness;
- the rigid/hinged joint approach where the gridshell is composed mostly by hinged joints and by a low number of rigid joints arranged in optimal positions, in order to avoid global buckling phenomena.

The proposed approaches are applied to a case study constituted by gridshells characterized by different boundary conditions, in order to investigate also the role of the restraint conditions on the global stiffness. The approaches have been also applied both to the perfect shape, i.e. that directly derived by a form-finding process, and to an imperfect shape, in order to analyze the role of geometrical imperfections.

2. Case study

The case study selected for developing the numerical simulations are the single layer gridshell structures analyzed in some recent literature works [16,19–21,23]. The gridshells are made of a square grid composed of nodes equally spaced in both directions. All the members of the canopies are composed of a hollow circular steel cross section with a

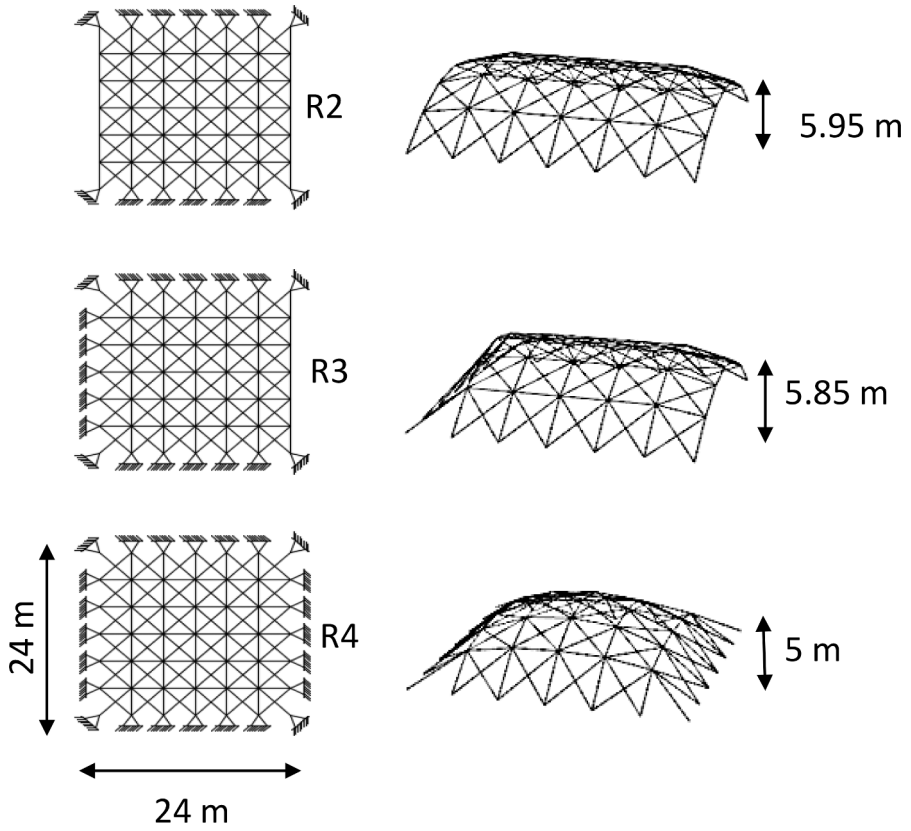

Fig. 2. Gridshell case studies: (a) R2 restrained on two sides; (b) R3 restrained on three sides; (c) R4 restrained on four sides.

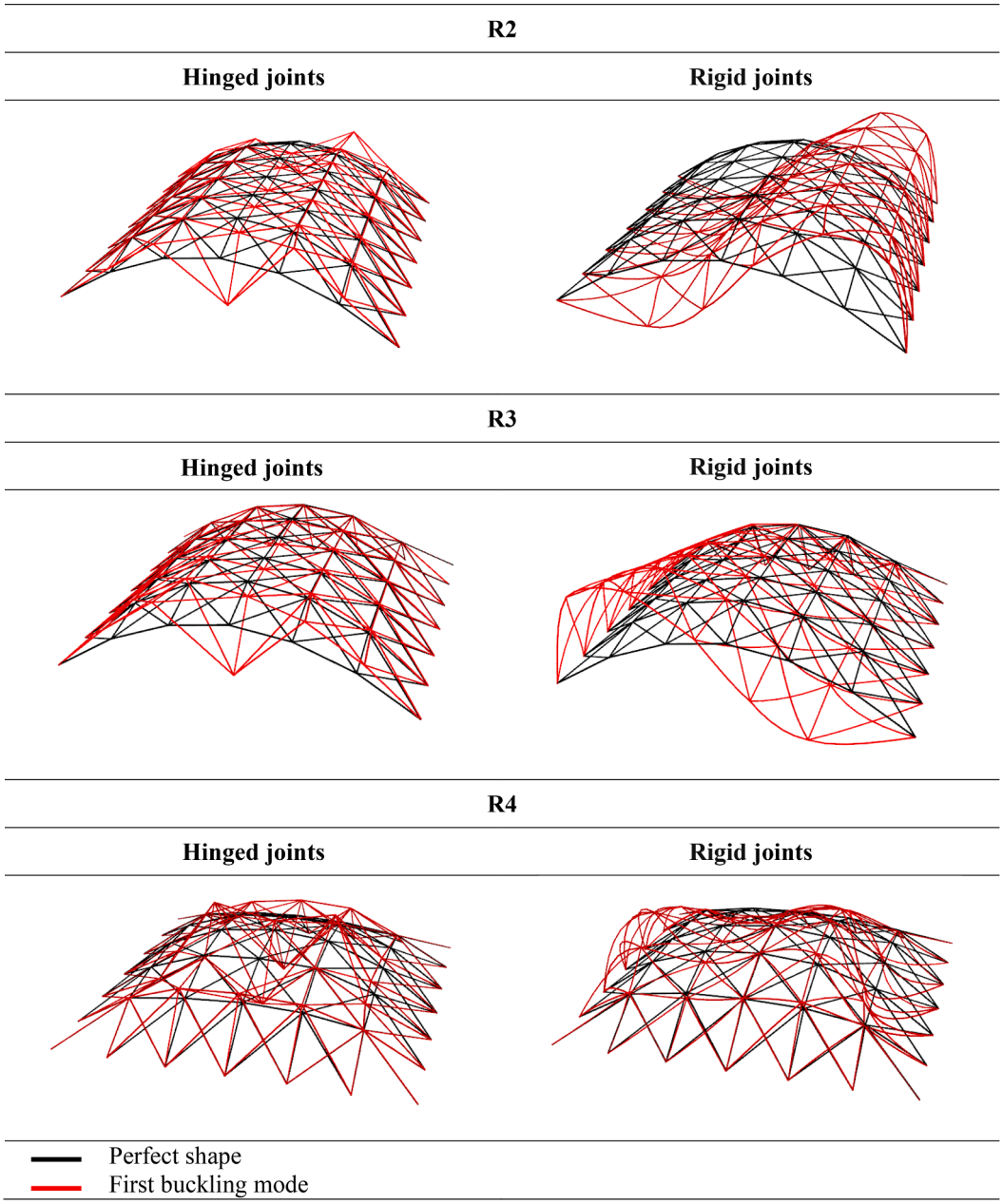

Fig. 3. First buckling mode for gridshells R2, R3, R4 with hinged and rigid joints.

S355 steel grade material (yield strength: 355 MPa; Young's modulus: 200 GPa), which diameter Φ is a variable to design, while the thickness *t* is set as 0.09 times the diameter. The design of the cross-sections has been performed by the proposed optimization strategies, that will be explained in section 3, by imposing structural requirements on the Buckling Factor BF $\geq$ 3, on the maximum displacement $D_{max} \leq$ limit displacement D_{lim}, imposed equal to L/250 (where L in the maximum span of the gridshell), and on the maximum value of utilization ratio $U_{max} \leq$ limit utilization ratio U_{lim}. In particular, U_{lim} is evaluated following the prescription of Eurocode 3 [44]:

$$U_{lim} = max\begin{cases} U_b = \begin{cases} if N > 0 : \dfrac{N}{N_{Rd}} + \left|\dfrac{M_y}{M_{y,Rd}}\right| + \left|\dfrac{M_z}{M_{z,Rd}}\right| \\ if N < 0 : -\dfrac{N}{N_{b,Rd}} + \left|\dfrac{M_y}{M_{y,Rd}}\right| + \left|\dfrac{M_z}{M_{z,Rd}}\right| \end{cases} \\ U_s = \left|\dfrac{V}{V_{y,Rd}}\right| + \left|\dfrac{V_z}{V_{z,Rd}}\right| \end{cases} \quad (1)$$

In details, U_b is the Utilization Ratio evaluated for normal forces and bending moments, where: N is the normal force, positive for tension and negative for compression; N_{Rd} is the resisting normal force; $N_{b,Rd}$ is the buckling force, evaluated following the prescription of Eurocode 3 [44]; M_y and M_z are the bending moments evaluated along the local y and z axis of the structural members (Fig. 1), respectively; $M_{y,Rd}$ and $M_{z,Rd}$ are the resisting bending moments evaluated along the local y and z axis of the members (Fig. 1), respectively; U_s is the Utilization Ratio evaluated

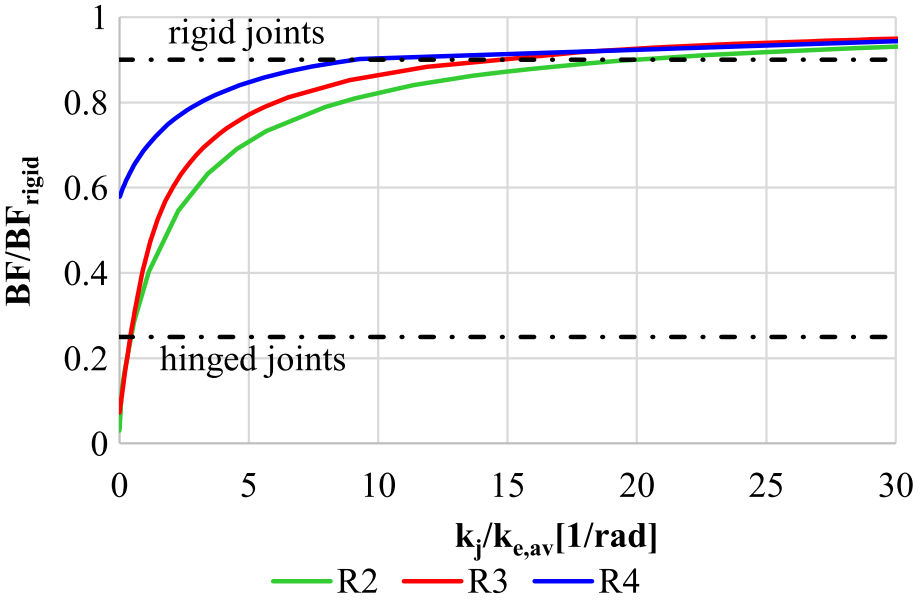

Fig. 4. Buckling Factor vs ratio between joint rotational stiffness k_j and element flexural stiffness $k_{e,av}$.

for shear forces, where V_y and V_z are the shear forces acting along the local y and z axis of the members (Fig. 1), respectively; $V_{y,Rd}$ and $V_{z,Rd}$ are the resisting shear forces evaluated along the local y and z axis of the members (Fig. 1), respectively.

Three different schemes of boundary conditions have been considered: (a) gridshell pin supported along two opposite sides (R2 – Fig. 2a); (b) gridshell pin supported along three sides (R3 – Fig. 2b); (c) gridshell pin supported along four sides (R4 – Fig. 2c).

For all the schemes, a uniform gravity load equal to 3 kN/m^2, including an estimate of the gridshell dead and live loads, has been considered, in analogy to previous literature works, for sake of comparison [16,45]. In particular, the dead load takes into account the structural weight of the steel members and the weight of the glass panels covering the gridshells, while the live load is referred to snow loads, for which a pressure of 0.8 kN/m^2 has been considered, typical of zone 2 in Italy, as defined by the Italian Standards [46]. The applied loads have been amplified by safety factors provided by Eurocode 1 [47].

The geometrical models have been developed within the software Grasshopper [48,49], i.e. an algorithmic-aided design tool based on visual scripting, that works in Rhinoceros [49] environment. The structural analyses have been carried out through Karamba [50,51], the Grasshopper plug-in for finite element analyses [48,49].

Furthermore, the three gridshells are characterized by the shape derived from a form-finding process, which has been performed by using the software Kangaroo [52], the Grasshopper physical engine where the Dynamic Relaxation method [53] is implemented. More in details, the adopted method is able to simulate the physical hanging model shape by treating all the structural elements and nodes as a particle spring system [54].

2.1. Preliminary analysis: the role of joint stiffness and restraint conditions

As already mentioned, the joints employed for single layer gridshells can be divided into three categories, on the basis of their stiffness [29]: rigid joints; semi-rigid joints and hinged joints. In particular, by considering the classification proposed by Fan et al. [29], a gridshell can be considered equipped with rigid joints if the stiffness of the joints guarantees the reaching of a buckling factor BF larger than 90 % of the BF reached in case of rigid joints; on the other hand, a gridshell can be considered equipped with hinged joints if the stiffness of the joints provides a buckling factor BF lower than 25 % of the BF reached in case of rigid joints. In all intermediate cases, the gridshell is considered equipped with semi-rigid joints. In order to introduce the effect of joint stiffness on the global behaviour of gridshells, Fig. 3 shows the first buckling mode, evaluated by Linear Buckling Analyses, of the R2, R3 and R4 configurations by considering hinged and rigid joints. From the plots it is evident how, for hinged joints, the buckling phenomena is mainly due to snap-trough instability, while for rigid joints, the buckling phenomena is due to a general instability [55]. It suggests that, in the first case, only a small number of structural elements reacts to buckling phenomena, while in the second case, the entire structure comes into play, so a greater safety against buckling is expected.

With reference to the three case studies, characterized by different restraint conditions (R2, R3 and R4 – Fig. 2), the trend of the buckling factor of the gridshell has been evaluated by varying the joint rotational stiffness k_j, under the condition of adopting a cross-section that guarantees an adequate buckling factor also in the case of hinged joints. To this purpose, Fig. 4 plots the ratio between the buckling factor BF of the gridshell structure and that BF_{rigid}, referred to the case of gridshell with rigid joints, in function of the ratio between the rotational stiffness of the joints k_j, evaluated in kNm/rad, and the average flexural stiffness of the elements $k_{e,av}$, evaluated, in kNm, by the following expression:

$$k_{e,av} = \frac{EI}{L_{av}} \tag{2}$$

where E is the Young modulus of steel, I is the moment of inertia of the cross-section, and L_{av} is the average length of elements.

In the same figure are also reported the thresholds of the ratio BF/BF_{rigid} suggested by Fan et al. [29] to classify the hinged and rigid joints, respectively equal to 0.25 and 0.9. From Fig. 4 emerges that the R2 case behaves as a gridshell with rigid joints for $k_j/k_{e,av}$ larger than 20, the R3 case for $k_j/k_{e,av}$ larger than 15, while the R4 case for $k_j/k_{e,av}$ larger than 8. On the other hand, the R2 and R3 cases behave as a gridshell with hinged joints for $k_j/k_{e,av}$ lower than 0.25, while the R4 case is characterized by a BF always larger than 0.58, which means that it never behaves as a gridshell equipped with hinged joints, also if it is effectively composed by hinged joints. These results highlight the great influence not only of the joint stiffness, but also of the boundary conditions, on the global behaviour of gridshells. It suggests that an adequate categorization of the joints cannot be performed a priori, since it also depends on external conditions. In this context, it is evident the usefulness to define

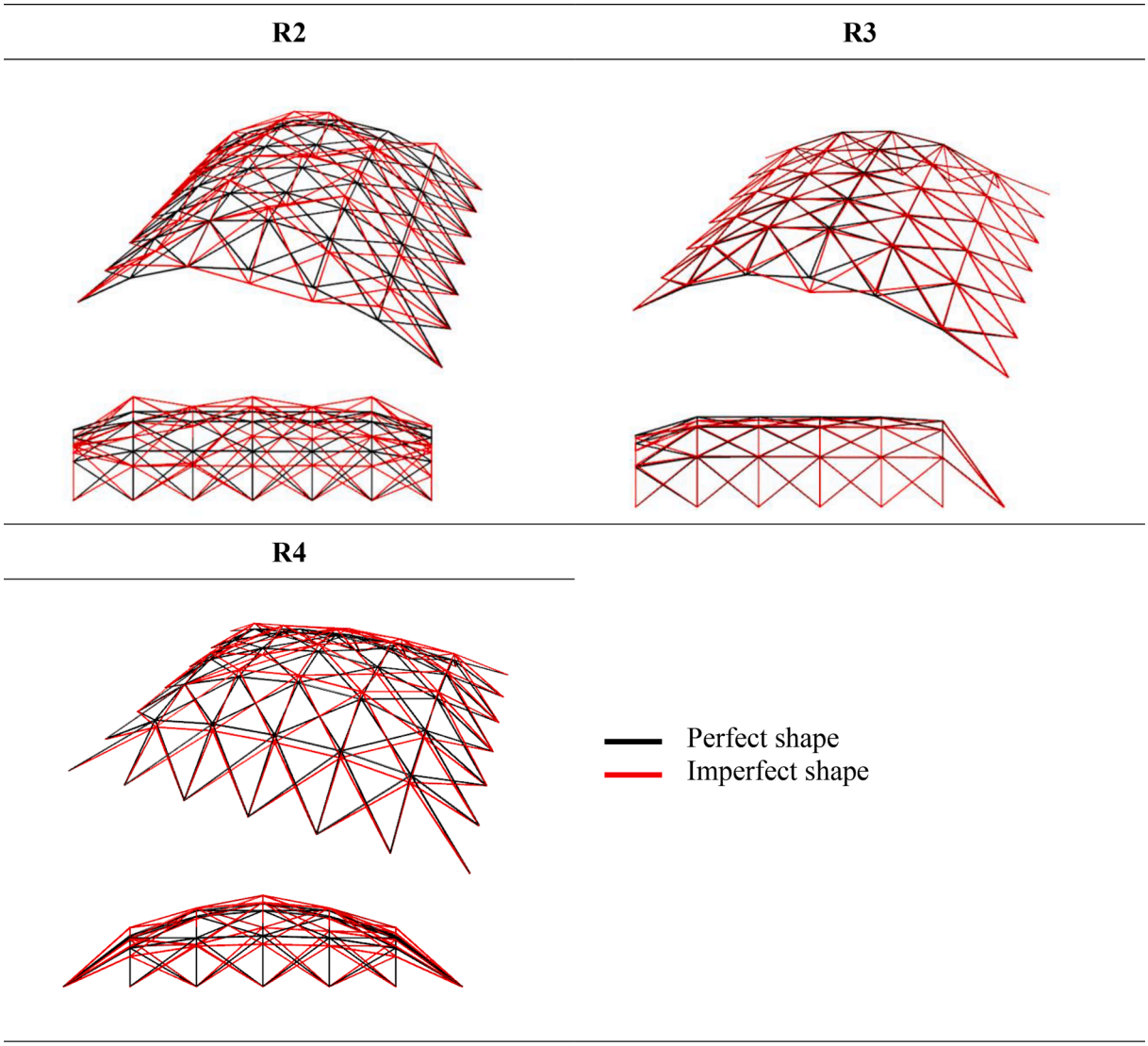

Fig. 5. Perfect shape vs imperfect shape (the imperfections are amplified).

design strategies capable of providing an adequate stiffness to the joints on the basis of external conditions, which is properly the aim of this paper.

3. The optimization approaches

In the context of structural optimization, some pioneering works propose to design the joints by means of a topology optimization process, from which particular configuration can be derived in function of the stress acting on the joints, which also depends on the required level of stiffness; furthermore, from a constructive point of view, these non-conventional joints can be simply built thought additive manufacturing techniques. In this framework, Zhu et al. [56] performed a multi-objective topology optimization for joints connecting six circular hollow cross-sections to employ in spatial-structures: starting from a spherical node, the optimal topology has been found by removing material, in order to minimize both the compliance and the first natural frequency. Seifi et al. [57] proposed a topology optimization of six-way structural nodes for triangulated gridshells composed of hollow rectangular cross-sections, by considering different load conditions; then the optimized joints have been realized by means of additive manufacturing. In a similar way, Wang et al. [58] proposed a topology optimization for spatial structures characterized by a quadrangular mesh and members with rectangular hollow cross-sections, which joints have to be realized by means of additive manufacturing. These strategies certainly represent a valid approach to design the node with the required level of stiffness, which could derive from a design process based on optimization approaches applied to the whole structure.

In this framework, the paper proposes and compares two optimization approaches, in order to obtain the minimum weight design of gridshell structures which also guarantee safety against global buckling phenomena: the joint stiffness approach and the rigid/hinged joint approach. The joint stiffness approach provides to find the optimal rotational stiffness to confer to all the joints of the gridshell, while the rigid/hinged joint approach aims to find a structural solution composed mostly of hinged joints and a small number of rigid ones, arranged in such a way as to minimize the structural weight. Both optimization problems are entrusted to a mono-objective genetic algorithm, which is implemented in the component Galapagos of Grasshopper [48,59]. The algorithms of this category are based on the natural selection concept: starting from a population of individuals randomly generated, where each individual is a potential solution, at each step the algorithm selects the best individuals (the parents) to mate or to mutate to produce children, i.e. the individuals of the next generation, until reaching a population of individuals which contains the optimal solution [60]. More in details, the main steps of Galapagos algorithm are: creation of

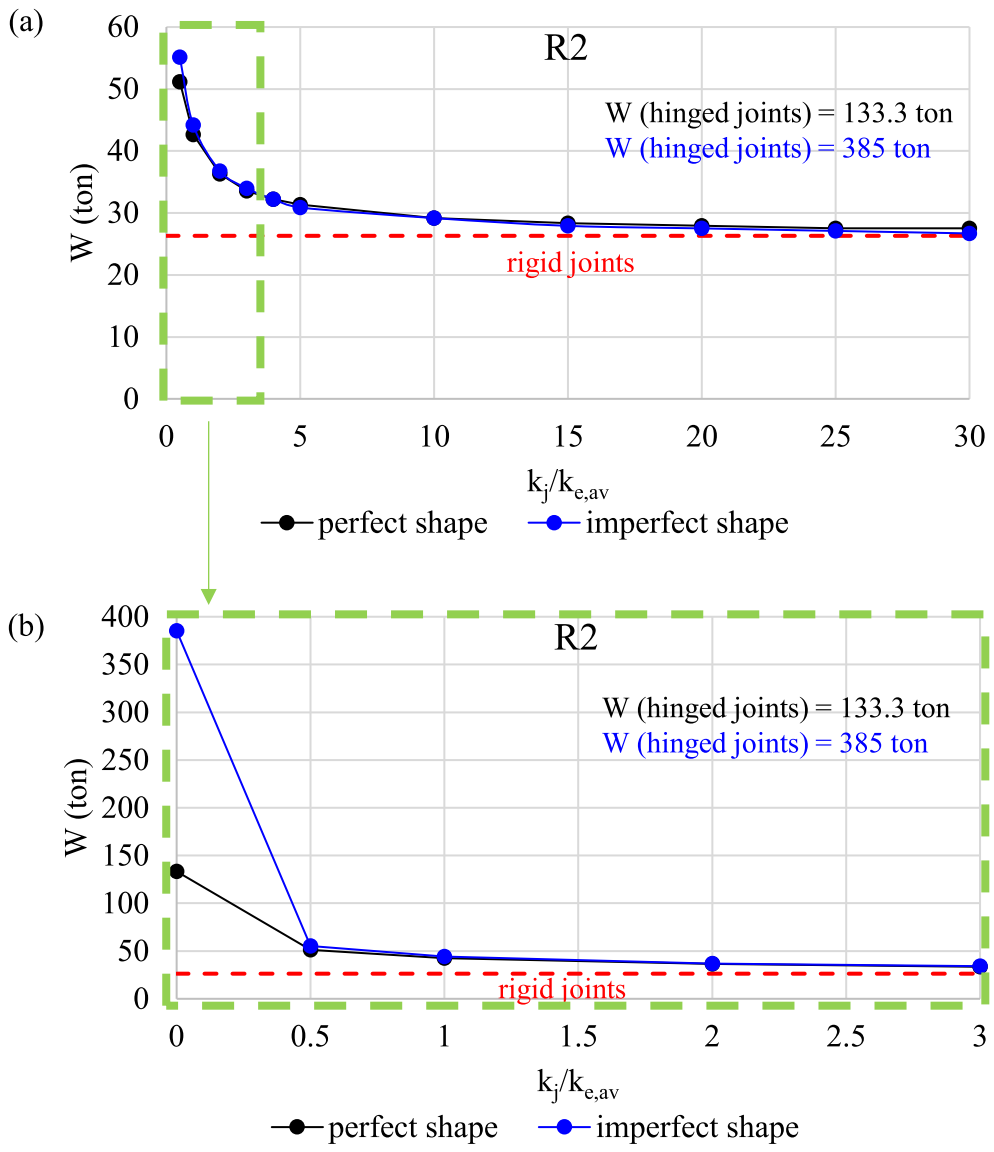

Fig. 6. Optimization problem results for gridshell R2: weight vs ratio between joint rotational stiffness k_j and element flexural stiffness $k_{e,av}$.

Table 1
Optimization problem results for gridshell R2.

R2 – perfect shape													
φ (cm)	29.7	18.4	16.8	15.5	14.9	14.6	14.4	13.9	13.7	13.6	13.5	13.5	13.2
$k_j/k_{e,av}$ (kNm)	0	0.5	1	2	3	4	5	10	15	20	25	30	∞
$k_{e,av}$ (kNm)	8459	1246	866	628	536	494	468	406	383	372	361	361	330
W (ton)	133	51	43	36	34	32	31	29	28	28	28	28	26
U_{max}	0.02	0.08	0.12	0.16	0.18	0.20	0.21	0.24	0.25	0.26	0.26	0.26	0.29
D_{max} (m)	0.001	0.002	0.003	0.003	0.003	0.003	0.003	0.003	0.003	0.003	0.003	0.003	0.003
BF	3	3	3	3	3	3	3	3	3	3	3	3	3
R2 – imperfect shape													
φ (cm)	50.5	19.1	17.1	15.6	15.0	14.6	14.3	13.8	13.6	13.5	13.4	13.3	13.1
$k_j/k_{e,av}$ (kNm)	0	0.5	1	2	3	4	5	10	15	20	25	30	∞
$k_{e,av}$ (kNm)	70,717	1447	930	644	550	494	455	406	372	361	351	340	320
W (ton)	385	55	44	37	34	32	31	29	28	28	27	27	26
U_{max}	0.01	0.09	0.13	0.18	0.20	0.21	0.24	0.25	0.28	0.29	0.30	0.31	0.30
D_{max} (m)	0.007	0.012	0.012	0.012	0.012	0.007	0.012	0.006	0.011	0.011	0.011	0.114	0.005
BF	3	3	3	3	3	3	3	3	3	3	3	3	3

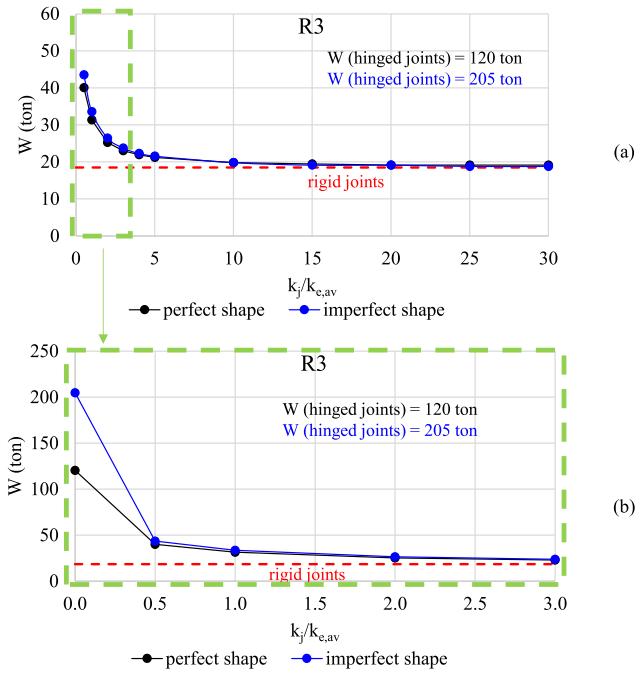

Fig. 7. Optimization problem results for gridshell R3: weight vs ratio between joint rotational stiffness k_j and element flexural stiffness $k_{e,av}$.

the first generation with random individuals; computation of the Objective Function, i.e. the quantity to minimize, for each individual of the current generation; selection of the best individuals (the parents) of the current generation to survive in the next one; selection of individuals to mate and to mutate to create the children of the next generation; the optimization process ends when the maximum number of generations is reached, there is no progress for a specified number of generations, or a specific fitness value is achieved.

3.1. The joint stiffness approach

The joint stiffness approach aims to provide the minimum weight design for gridshells, by varying the rotational stiffness of the joints and the cross-sections to assign to the elements. In particular, the optimization process is defined as in the following:

for each $k_j/k_{e,av}$

Minimize W

Subjected to $BF \geq BF_{lim}$

$U_{max} \leq U_{lim}$

$D_{max} \leq D_{lim}$

$\Phi_{lb} \leq \Phi \leq \Phi_{ub}$ (3)

VariableΦ

where: W is the structural weight of the gridshell, BF and BF_{lim} are the actual and the limit buckling factor value, respectively; U_{max} and U_{lim} are the maximum and the limit utilization factor, respectively; D_{max} and D_{lim} are the maximum and the limit displacement, respectively; Φ_{lb} and Φ_{ub} are the lower and upper bound values of the diameter Φ, respectively. The limit value of the buckling factor BF_{lim} have been imposed equal to 3; the limit value of utilization U_{lim} is set equal to 1; limit value of displacement D_{max} is set equal to 0.096 m, i.e. the maximum span L divided by 250; Φ_{lb} and Φ_{ub} are equal to 5 cm and 20 cm, respectively.

The optimization process has been applied both to the perfect shape, i.e. that directly derived by the form-finding process, and to an imperfect shape, which takes into account geometrical imperfections. In particular, the last one has been derived by an optimization process proposed by Tomei et al. [22] based on genetic algorithms, finalized to minimize the BF by varying the coordinates of the joints in the range ± 0.05 m (L/500), which is the amplitude of imperfections, with respect to the perfect configuration. More in details, the formulation of the optimization problem is stated as:

Minimize BF

$$\text{Subjected to} -\frac{L}{500} \leq \sqrt{(x_{fj}-x_{0j})^2+(y_{fj}-y_{0j})^2+(z_{fj}-z_{0j})^2} \leq +\frac{L}{500}$$

Variables : x_{fj}, y_{fj}, z_{fj} (4)

where x_{fj}, y_{fj}, and z_{fj} are the three coordinates of the *jth* node of the imperfect gridshells, while x_{0j}, y_{0j}, and z_{0j} are the three coordinates of the *jth* node of the perfect ones. Although different literature works suggest several methods to select a proper shape of imperfections [32,61–69], other works show that the one generated with the optimization method employed by Tomei et al. [22] provides the worst Buckling Factor compared to other ones, so this methods has been selected to apply imperfections. At title of example, Fig. 5 shows the imperfect shape overlapped to the perfect one, for R2, R3 and R4 cases.

The maximum amplitude of imperfections has been set equal to L/500 according to the recommendations of previous literature works [65,70].

Table 2
Optimization problem results for gridshell R3.

R3 – perfect shape													
φ (cm)	28.6	16.5	14.6	13.1	12.5	12.2	12.0	11.6	11.5	11.4	11.4	11.4	11.2
$k_j/k_{e,av}$ (kNm)	0	0.5	1	2	3	4	5	10	15	20	25	30	∞
$k_{e,av}$ (kNm)	7050	781	479	310	257	233	219	191	184	178	178	178	166
W (ton)	120	40	31	25	23	22	21	20	19	19	19	19	18
U_{max}	0.02	0.15	0.23	0.35	0.42	0.46	0.49	0.56	0.58	0.60	0.60	0.60	0.64
D_{max} (m)	0.001	0.003	0.003	0.004	0.004	0.004	0.004	0.005	0.005	0.005	0.005	0.005	0.005
BF	3	3	3	3	3	3	3	3	3	3	3	3	3
R3 – *imperfect shape*													
φ (cm)	37.3	17.2	15.1	13.4	12.7	12.3	12.1	11.6	11.5	11.4	11.3	11.3	11.2
$k_j/k_{e,av}$ (kNm)	0	0.5	1	2	3	4	5	10	15	20	25	30	∞
$k_{e,av}$ (kNm)	20,398	922	548	340	274	241	226	191	178	178	172	172	166
W (ton)	205	44	34	26	24	22	22	20	19	19	19	19	18
U_{max}	0.02	0.14	0.22	0.34	0.42	0.47	0.50	0.59	0.63	0.62	0.65	0.65	0.67
D_{max} (m)	0.013	0.013	0.013	0.012	0.011	0.011	0.010	0.009	0.008	0.007	0.007	0.007	0.006
BF	3	3	3	3	3	3	3	3	3	3	3	3	3

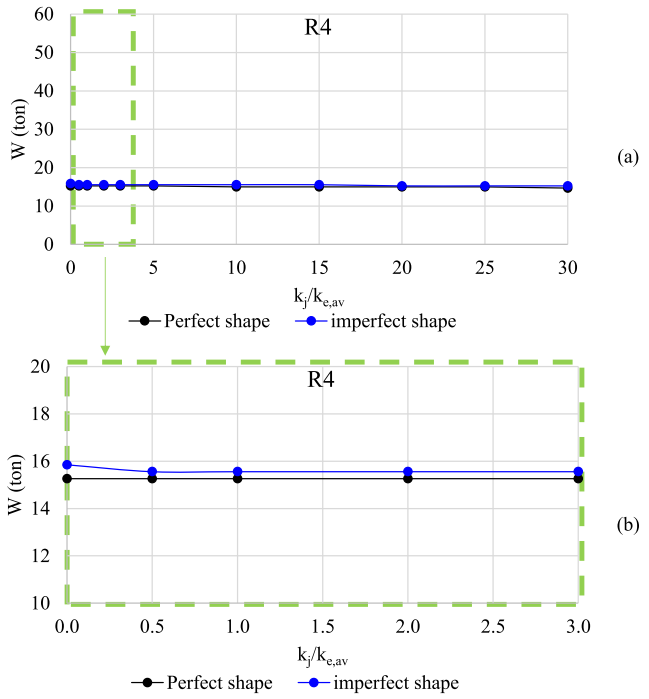

Fig. 8. Optimization problem results for gridshell R4: weight vs ratio between joint rotational stiffness k_j and element flexural stiffness $k_{e,av}$.

Fig. 6 shows the minimum weight obtained for the gridshell R2 from the optimization process in function of the ratio $k_j/k_{e,av}$; it is evident that the weight greatly decreases by increasing the ratio $k_j/k_{e,av}$ from zero (hinged joints) to 5 (Fig. 6a), while the reduction becomes less evident for $k_j/k_{e,av}$ greater to 5, for which the weight approaches the one obtained in the case of rigid joints. Furthermore, in the case of hinged joints (zero joint stiffness), the imperfections lead to an increase of the weight of 2.9 times with respect to the perfect shape, although this difference quickly reduces by increasing the ratio $k_j/k_{e,av}$ (Fig. 6b). This result indicates that even a small increase in rotational stiffness of the joints, with respect to the configuration of zero stiffness, greatly reduces the sensitivity of the gridshell to imperfections. Table 1 shows the results of all the optimization processes, for both perfect and imperfect shapes, also in terms of U_{max}, D_{max} and BF: in all cases, the BF reaches its limit value, while U_{max} and D_{max} are always lower than U_{lim} and D_{lim}, respectively, meaning that the design is always governed by the sensitivity of the gridshell to global buckling phenomena.

Fig. 7 and Table 2 show the results for the gridshell R3: this case confirms the previous considerations, but it is interesting to observe that the weights obtained for R2 are always larger than that obtained for R3. In particular, by considering the perfect shapes, the R2 gridshell is characterized by a weight greater than 47 % of that of the gridshell R3; furthermore, by considering the imperfect shapes, the R2 gridshell is characterized by a weight greater than 88 % of that of the gridshell R3.

Fig. 8 and Table 3 show the results for the gridshell R4: unlike the other cases, a negligible variation of weight is observed as the stiffness ratio increases, and there is no substantial difference either between the weight obtained with the perfect shape and the imperfect one. This result suggests that, in the case of R4 configuration, the global behaviour is independent from the joint stiffness, and almost independent from imperfections, since the restraint conditions assures an adequate stiffness to the whole structure. Comparing the results in terms of weight with respect to the other configurations, the R4 gridshell is characterized by a weight lower than 23 % and 67 % of gridshells R3 and R2 (perfect shape), respectively.

This result highlights the influence of the boundary conditions on the susceptibility to global buckling phenomena: as it is expected, the greater the number of the restrained sides, the lower the optimal weight. This concept is immediately evident by observing Fig. 9, in which the results in terms of weight for the R2, R3 and R4 configurations are compared. These plots are the same reported from Fig. 6 to Fig. 8 for the perfect configuration, here overlapped for sake of comparison. In particular, the minimum weight W, obtained from the optimization processes, is reported in function of the joint rotational stiffness ratio $k_j/k_{e,av}$, in reference to the cross-section obtained from optimization and also reported in Table 1, Table 2 and Table 3 for R2, R3 and R4

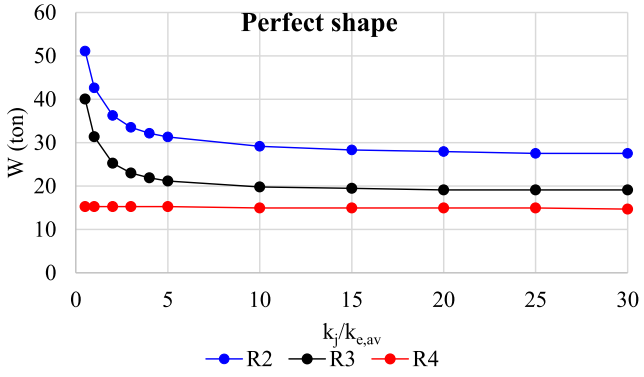

Fig. 9. Comparison between optimization problem results for gridshell R2, R3, R4 and perfect shape: weight vs ratio between joint rotational stiffness k_j and element flexural stiffness $k_{e,av}$.

Table 3
Optimization problem results for gridshell R4.

R4 – perfect shape													
φ (cm)	10.6	10.6	10.6	10.6	10.6	10.6	10.6	10.5	10.5	10.5	10.5	10.4	9.3
$k_j/k_{e,av}$ (kNm)	0	0.5	1	2	3	4	5	10	15	20	25	30	∞
$k_{e,av}$ (kNm)	136	136	136	136	136	136	136	131	131	131	131	126	80
W (ton)	15	15	15	15	15	15	15	15	15	15	15	15	12
U_{max}	0.45	0.45	0.45	0.45	0.45	0.45	0.45	0.46	0.46	0.46	0.46	0.48	0.74
D_{max} (m)	0.005	0.005	0.005	0.005	0.005	0.005	0.005	0.005	0.005	0.005	0.005	0.005	0.006
BF	3	3	3	3	3	3	3	3	3	3	3	3	3
R4 – imperfect shape													
φ (cm)	10.8	10.7	10.7	10.7	10.7	10.7	10.7	10.7	10.7	10.6	10.6	10.6	9.3
$k_j/k_{e,av}$ (kNm)	0	0.5	1	2	3	4	5	10	15	20	25	30	∞
$k_{e,av}$ (kNm)	146	141	141	141	141	141	141	141	141	136	136	136	80
W (ton)	16	16	16	16	16	16	16	16	16	15	15	15	12
U_{max}	0.44	0.46	0.46	0.46	0.46	0.46	0.46	0.46	0.46	0.47	0.47	0.47	0.74
D_{max} (m)	0.006	0.006	0.006	0.006	0.006	0.006	0.006	0.006	0.006	0.006	0.006	0.006	0.006
BF	3	3	3	3	3	3	3	3	3	3	3	3	3

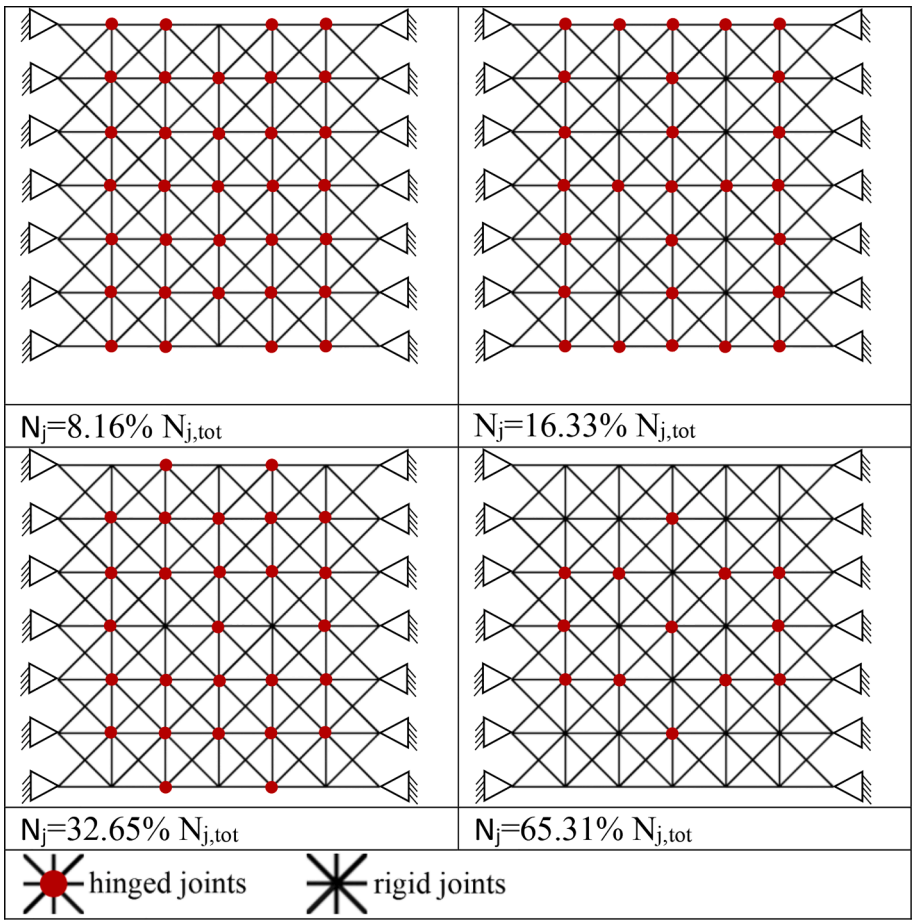

Fig. 10. Rigid/Hinged joint optimization approach: arrangement of rigid joints.

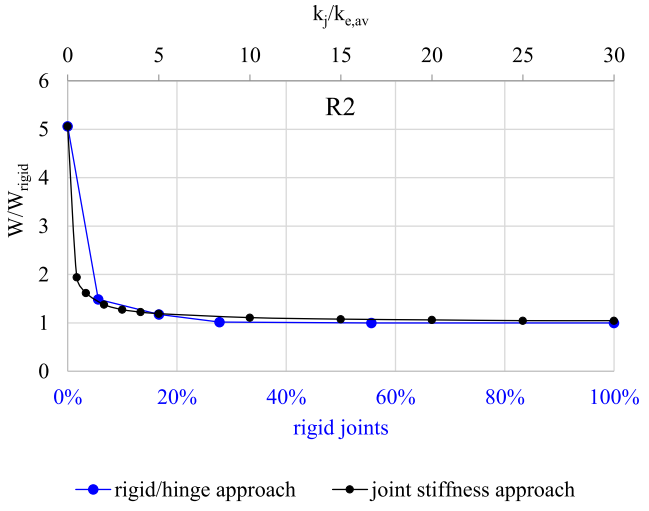

Fig. 11. Comparison between the optimization approaches for gridshell R2: weight vs ratio between $k_j/k_{e,av}$ (joint stiffness approach); weight vs percentage of rigid joints (rigid/ hinged joint approach).

configurations, respectively.

These results highlight how both the boundary conditions and the stiffness of the joints play a fundamental role in determining the global stiffness of the structure.

3.2. The Rigid/Hinged joint approach

The rigid/ hinged joint approach aims to optimize the position of a certain number of rigid joints, while all the other ones are hinged [22,23]. Also in this case, the objective is to minimize the weight, by varying the cross-sections of the elements and the position of a certain number of rigid joints. In particular, the optimization process is defined as in the following:

For each *percentage of rigid joints*

Minimize W

Subjected to $BF \geq BF_{lim}$

$$U_{max} \leq U_{lim} \quad (5)$$

$D_{max} \leq D_{lim}$

$\Phi_{lb} \leq \Phi \leq \Phi_{ub}$

Variables Φ, position of rigid joints

Fig. 10 shows the arrangement of the rigid joints obtained from the optimization process for different percentages of rigid joints. The obtained solutions are characterized by the majority of rigid joints located along or in proximity of the free edges of the gridshell, thus stiffening the most deformable part of the structure. The results in terms of W/W_{rigid}, where W_{rigid} is referred to the minimum weight found by imposing all rigid joints, in function of the percentage of the rigid joints are reported in blue in Fig. 11. The figure shows that just a low percentage of rigid

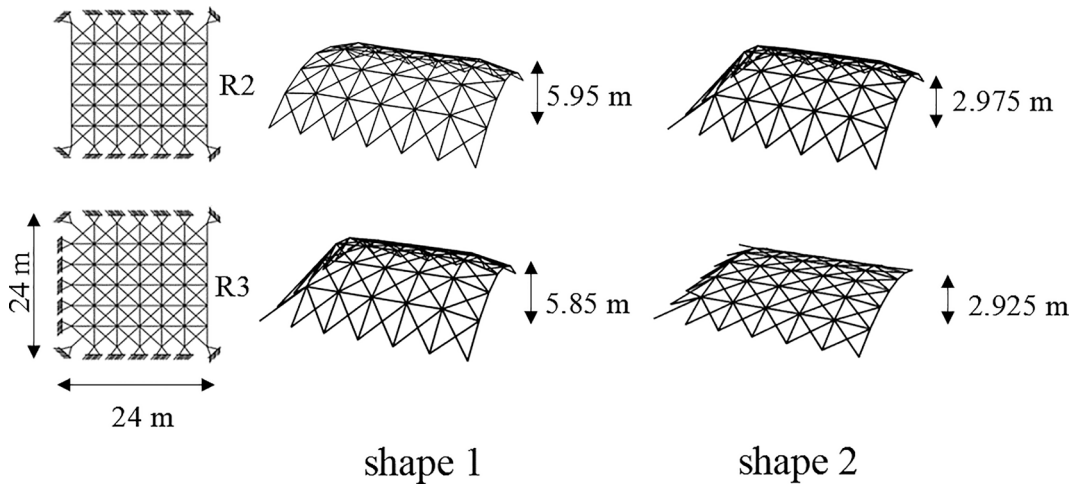

Fig. 12. Gridshell case studies: shape 1 vs shape 2.

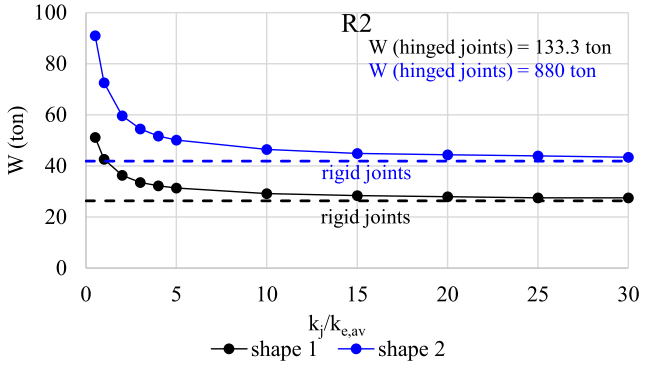

Fig. 13. Optimization problem results for gridshell R2: weight vs ratio between joint rotational stiffness k_j and element flexural stiffness $k_{e,av}$ for shape 1 and shape 2.

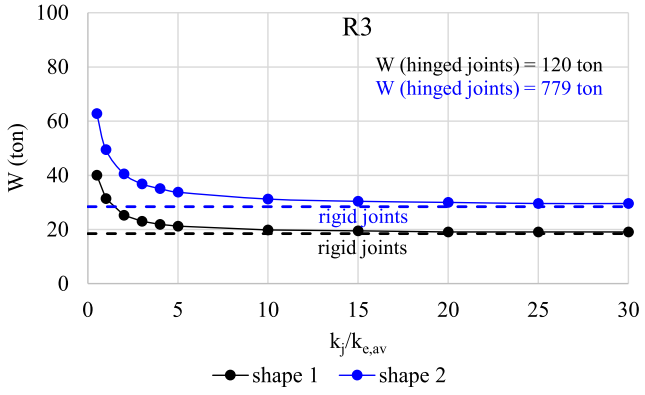

Fig. 14. Optimization problem results for gridshell R2: weight vs ratio between joint rotational stiffness k_j and element flexural stiffness $k_{e,av}$ for shape 1 and shape 2.

joints allows to greatly reduce the structural weight of the gridshell. In the same graph is also reported, for sake of comparison, the W/W_{rigid} vs $k_j/k_{e,av}$ obtained by the joint stiffness approach, from which also emerge the fast reduction of the structural weight by increasing the joint rotational stiffness. Actually, the two curves are quite overlapping since the two approaches let to reach the same level of weight; this result suggests that both the approaches are effective for the minimum weight design of gridshells, with the respect of the safety condition towards global buckling phenomena.

4. The role of the shape

One of the most key features which makes gridshells fascinating structures is the possibility of giving them particular shapes, which do not only affect the aesthetic/architectural features but also, and meaningfully, the structural aspects, being the shape the structure itself. In order to analyse the structural meaning of the shape, the proposed joint stiffness approach has been applied to the gridshells R2 and R3 characterized by a shape derived by a form-finding process and characterized by a maximum height reduced of 50 % (Fig. 12 – shape 2) with respect to the solutions already described in section 2 (Fig. 2 and Fig. 12 – shape 1).

The results in terms of W vs $k_j/k_{e,av}$ for the two shapes 1 and 2 are shown in Fig. 13 and Fig. 14 for gridshells R2 and R3, respectively. In both cases, the trend of the two curves is similar, but shapes 2 provide larger values of weight. The difference in terms of weight reduces by increasing the ratio $k_j/k_{e,av}$, going from about 650 % in case of hinged joints until 150 % in case of rigid joints. This difference is due to the fact that the shape 1 is characterized by a lower curvature than shape 2, which leads the gridshell toward a “dome” behaviour where the grid elements work predominantly in compression; on the other hand, shape 2 is characterized by a higher curvature than shape 1, which leads the gridshell toward a “plate” behaviour where the grid elements work in bending rather than compression. Since the bending stiffness of a slender beam is much less than its axial stiffness, it is clear that if the elements are forced to work in bending, higher cross-section sizes are required. This result highlights the relevant structural meaning of the shape, and its role in conceiving minimum weight solutions.

5. Conclusions

The paper presents two structural optimization approaches for the minimum weight design of gridshell structures, by specifically taking into account the role of joint rotational stiffness, which strongly affects the susceptibility to global buckling. In particular, the first approach, named the “joint stiffness approach”, considers the gridshell composed by semi-rigid joints characterized by the same rotational stiffness; the second approach, named the “rigid/hinged approach”, considers a hinged-joint gridshell equipped by a low number of rigid joints arranged in optimal positions in order to assure the minimum weight solution. Furthermore, the optimization approaches have been applied to case studies characterized by different boundary conditions, different rise-to-span ratios and in case of perfect and imperfect shapes, in order to also

analyse the effect of imperfections, which could arise during the construction process.

On the basis of the discussed analyses, it is possible to outline the following considerations on the structural behavior of the gridshells to be considered during the design phase:

- the results of the proposed optimization processes highlight the beneficial effect of a finite value of the rotational stiffness of the joints, also if small, in the susceptibility of the gridshell to global buckling phenomena; in particular, it leads to a strong increase of the BF with respect to the configuration of hinged joints, which allows to use smaller cross-sections, in order to reduce the weight;
- the presence of a finite value of the rotational stiffness of the joints, also if small, reduces the sensitivity of the BF of the gridshells to geometrical imperfections;
- the previous considerations are confirmed by also considering structural solutions characterized by the most part of hinged joints, and equipped with a small number of rigid joints;
- the boundary conditions strongly affect the susceptibility of the gridshell to global buckling phenomena; indeed, the lower the number of restrained sides, the higher the structural weight necessary to assure an adequate stiffness against buckling phenomena;
- the shape assumes a fundamental role on the structural behaviour of gridshells, indeed, as the curvature decreases, the gridshell tends to behave like a “dome”, so bending in structural elements becomes negligible; this leads to decreasing cross-sections and therefore to a lower structural weight compared to a gridshell characterized by a high curvature.

Further developments could be to apply the proposed strategies to gridshells characterized by different plan shape and different meshes, such as quadrangular ones, in order to extend the validity of the previous considerations to different gridshell typologies.

Declaration of Competing Interest

The authors declare that they have no known competing financial interests or personal relationships that could have appeared to influence the work reported in this paper.

References

[1] Pugnale A, Echenagucia TM, Sassone M. Computational morphogenesis: design of freeform surfaces. Shell Struct Archit Form Find Optim, Routledge 2014:225–36. https://doi.org/10.4324/9781315849270-28.

[2] Donofrio M. Topology optimization and advanced manufacturing as a means for the design of sustainable buildings components. Procedia Eng 2016;145:638–45.

[3] Beghini A, Sarkisian M. Geometry optimization in structural design. Struct Eng Assoc Calif 83rd Annu Conv Proceeding 2014.

[4] Sarkisian M, Lee P, Long E, Shook D. Organic and natural forms in building design. Struct Congr 2010, 2010.. https://doi.org/10.1061/41130(369)257.

[5] Stromberg LL, Beghini A, Baker WF, Paulino GH. Application of layout and topology optimization using pattern gradation for the conceptual design of buildings. Struct Multidiscip Optim 2011. https://doi.org/10.1007/s00158-010-0563-1.

[6] Stromberg LL, Beghini A, Baker WF, Paulino GH. Topology optimization for braced frames: Combining continuum and beam/column elements. Eng Struct 2012;37:106–24. https://doi.org/10.1016/j.engstruct.2011.12.034.

[7] Tomei V, Imbimbo M, Mele E. Optimization of structural patterns for tall buildings: The case of diagrid. Eng Struct 2018;171. https://doi.org/10.1016/j.engstruct.2018.05.043.

[8] Mele E, Imbimbo M, Tomei V. The effect of slenderness on the design of diagrid structures. Int J High-Rise Build 2019. 10.21022/IJHRB.2019.8.2.83.

[9] Cascone F, Faiella D, Tomei V, Mele E. Stress lines inspired structural patterns for tall buildings. Eng Struct 2021;229:111546. https://doi.org/10.1016/j.engstruct.2020.111546.

[10] Chatzikonstantinou I, Ekici B, Sariyildiz IS, Koyunbaba BK. Multi-objective diagrid façade optimization using differential evolution. 2015 IEEE Congr. Evol. Comput. CEC 2015 – Proc., Institute of Electrical and Electronics Engineers Inc.; 2015, p. 2311–8. 10.1109/CEC.2015.7257170.

[11] Sgambi L, Gkoumas K, Bontempi F. Genetic Algorithms for the Dependability Assurance in the Design of a Long-Span Suspension Bridge. Comput Civ Infrastruct Eng 2012;27:655–75. https://doi.org/10.1111/j.1467-8667.2012.00780.x.

[12] Torii AJ, Lopez RH, Biondini F. An approach to reliability-based shape and topology optimization of truss structures. Eng Optim 2012;44:37–53. https://doi.org/10.1080/0305215X.2011.558578.

[13] Quinn G. Structural analysis for the pneumatic erection of elastic gridshells. Structures 2020;28:2276–90. https://doi.org/10.1016/j.istruc.2020.10.012.

[14] Biondini F, Bontempi F, Malerba PG. Fuzzy reliability analysis of concrete structures. Comput Struct 2004. https://doi.org/10.1016/j.compstruc.2004.03.011.

[15] Cascone F, Faiella D, Tomei V, Mele E. A Structural Grammar Approach for the Generative Design of Diagrid-Like Structures. Build 2021, Vol 11, Page 90 2021;11:90. 10.3390/BUILDINGS11030090.

[16] Richardson JN, Adriaenssens S, Filomeno Coelho R, Bouillard P. Coupled form-finding and grid optimization approach for single layer grid shells. Eng Struct 2013. https://doi.org/10.1016/j.engstruct.2013.02.017.

[17] Feng RQ, Ge JM. Shape optimization method of free-form cable-braced grid shells based on the translational surfaces technique. Int J Steel Struct 2013;13:435–44. https://doi.org/10.1007/s13296-013-3004-3.

[18] Kociecki M, Adeli H. Shape optimization of free-form steel space-frame roof structures with complex geometries using evolutionary computing. Eng Appl Artif Intell 2015. https://doi.org/10.1016/j.engappai.2014.10.012.

[19] Grande E, Imbimbo M, Tomei V. A two-stage approach for the design of grid shells. Struct Archit - Proc 3rd Int Conf Struct Archit ICSA 2016 2016.

[20] Grande E, Imbimbo M, Tomei V. Role of global buckling in the optimization process of grid shells: Design strategies. Eng Struct 2018;156. https://doi.org/10.1016/j.engstruct.2017.11.049.

[21] Grande E, Imbimbo M, Tomei V. Structural Optimization of Grid Shells: Design Parameters and Combined Strategies. J Archit Eng 2018;24. https://doi.org/10.1061/(ASCE)AE.1943-5568.0000286.

[22] Tomei V, Grande E, Imbimbo M. Influence of geometric imperfections on the efficacy of optimization approaches for grid-shells. Eng Struct 2021;228:111502. https://doi.org/10.1016/j.engstruct.2020.111502.

[23] Grande E, Imbimbo M, Tomei V. Optimization Strategies for Grid Shells: The Role of Joints. J Archit Eng 2020. https://doi.org/10.1061/(ASCE)AE.1943-5568.0000375.

[24] Teranishi M, Ishikawa K. Grid patterns optimization for single-layer latticed domes. Adv Struct Eng 2021;24:359–69. https://doi.org/10.1177/1369433220956813.

[25] Tomei V, Grande E, Imbimbo M. Influence of pretensioned rods on structural optimization of grid shells. In: Magd Abdel Wahab, editor. Proc. 4th Int. Conf. Numer. Model. Eng. Lect. Notes Civ. Eng., Singapore: Springer; 2022. 10.1007/978-981-16-8185-1.

[26] Tomei V, Grande E, Imbimbo M. Design optimization of gridshells equipped with pre-tensioned rods. J Build Eng 2022;52:104407. https://doi.org/10.1016/J.JOBE.2022.104407.

[27] Venuti F, Bruno L. Influence of in-plane and out-of-plane stiffness on the stability of free-edge gridshells: A parametric analysis. Thin-Walled Struct 2018;131:755–68. https://doi.org/10.1016/j.tws.2018.07.019.

[28] Venuti F. Influence of pattern anisotropy on the structural behaviour of free-edge single-layer gridshells. Curved Layer Struct 2021;8:119–29. https://doi.org/10.1515/cls-2021-0011.

[29] Fan F, Ma H, Cao Z, Shen S. A new classification system for the joints used in lattice shells. Thin-Walled Struct 2011;49:1544–53. https://doi.org/10.1016/J.TWS.2011.08.002.

[30] Lopez A, Puente I, Aizpurua H. Experimental and analytical studies on the rotational stiffness of joints for single-layer structures. Eng Struct 2011;33:731–7. https://doi.org/10.1016/J.ENGSTRUCT.2010.11.023.

[31] López A, Puente I, Serna MA. Numerical model and experimental tests on single-layer latticed domes with semi-rigid joints. Comput Struct 2007;85:360–74. https://doi.org/10.1016/J.COMPSTRUC.2006.11.025.

[32] Kato S, Mutoh I, Shomura M. Collapse of semi-rigidly jointed reticulated domes with initial geometric imperfections. J Constr Steel Res 1998. https://doi.org/10.1016/S0143-974X(98)00199-0.

[33] Wang X, Feng R, qiang, Yan G rong, Liu F cheng, Xu W jia.. Effect of joint stiffness on the stability of cable-braced grid shells. Int J Steel Struct 2016.1123–33.;2016(164):16. https://doi.org/10.1007/S13296-016-0041-8.

[34] Feng R, Yao B, Ye J. The Stability of Elliptic Paraboloid Grid Shell Lighting Roofs with Semi-Rigid Joints. Adv Mater Res 2012;374–377:2148–51. https://doi.org/10.4028/WWW.SCIENTIFIC.NET/AMR.374-377.2148.

[35] Zhang Z, Feng R. Experimental and numerical study on the hysteretic behaviour of double-ring joints under cyclic moments. J Constr Steel Res 2021;187:106939. https://doi.org/10.1016/J.JCSR.2021.106939.

[36] Han Q, Liu Y, Xu Y. Stiffness characteristics of joints and influence on the stability of single-layer latticed domes. Thin-Walled Struct 2016;107:514–25. https://doi.org/10.1016/J.TWS.2016.07.013.

[37] Han Q, Liu Y, Zhang J, Xu Y. Mechanical behaviors of the Assembled Hub (AH) joints subjected to bending moment. J Constr Steel Res 2017;138:806–22. https://doi.org/10.1016/J.JCSR.2017.08.026.

[38] Fan F, Ma H, Chen G, Shen S. Experimental study of semi-rigid joint systems subjected to bending with and without axial force. J Constr Steel Res 2012;68:126–37. https://doi.org/10.1016/J.JCSR.2011.07.020.

[39] Ma H, Ren S, Fan F. Experimental and numerical research on a new semi-rigid joint for single-layer reticulated structures. Eng Struct 2016;126:725–38. https://doi.org/10.1016/J.ENGSTRUCT.2016.08.028.

[40] Gidófalvy K, Ma H, Katula LT. Numerical Modelling of a Novel Joint System for Grid Shells with T Cross-sections. Period Polytech Civ Eng 2017;61:958–71. https://doi.org/10.3311/PPCI.9346.

[41] Tsavdaridis KD, Feng R, Liu F. Shape Optimization of Assembled Single-Layer Grid Structure with Semi-Rigid Joints. Procedia Manuf 2020;44:12–9. https://doi.org/10.1016/J.PROMFG.2020.02.199.
[42] Liu H, Ding Y, Chen Z. Static stability behavior of aluminum alloy single-layer spherical latticed shell structure with Temcor joints. Thin-Walled Struct 2017;120:355–65. https://doi.org/10.1016/J.TWS.2017.09.019.
[43] Yang L, Wang M, Wei S, Yu S. Rotating performance of Temcor joints for aluminum single-layer reticulated shells. Structures 2021;34:1346–63. https://doi.org/10.1016/J.ISTRUC.2021.08.038.
[44] European Committee for Standardization. EN 1993–1-1: Eurocode 3: Design of Steel Structures—Part 1–1: General Rules and Rules for Buildings 2005.
[45] Adriaenssens S, Block P, Veenendaal D, Williams C. Shell structures for architecture: Form finding and optimization. Shell Struct Archit Form Find Optim 2014;9781315849270:1–323. https://doi.org/10.4324/9781315849270.
[46] Transport M of I and. Aggiornamento delle "Norme Tecniche per le Costruzioni" (in Italian). Ministerial Decree 17 January 2018. 2018.
[47] Eurocode 2010;1. Actions on structures.
[48] Rutten D. Grasshopper: generative modeling for Rhino 2007.
[49] McNeel R. RHINOCEROS: NURBS modeling for Windows n.d.
[50] Preisinger C. Parametric structural modeling. Karamba 2013;3D.
[51] Preisinger C. Linking structure and parametric geometry. Archit Des 2013. https://doi.org/10.1002/ad.1564.
[52] Piker D. Kangaroo: Form finding with computational physics. Archit Des 2013;83:136–7. https://doi.org/10.1002/ad.1569.
[53] Day AS. An introduction to dynamic relaxation. Engineer 1965;219:218–21.
[54] Kilian A, Ochsendorf J. Particle Spring Models for form finding. J Int Assoc SHELL Spat Struct IASS 2005;VOL. 46.
[55] Gioncu V. Buckling of Reticulated Shells: State-of-the-Art. Int J Sp Struct 1995. https://doi.org/10.1177/026635119501000101.
[56] Zhu N, Liu J. Multiobjective Topology Optimization of Spatial-Structure Joints. Adv. Civ Eng 2021; 2021.. https://doi.org/10.1155/2021/5530644.
[57] Seifi H, Rezaee Javan A, Xu S, Zhao Y, Xie YM. Design optimization and additive manufacturing of nodes in gridshell structures. Eng Struct 2018;160:161–70. https://doi.org/10.1016/J.ENGSTRUCT.2018.01.036.
[58] Wang X, Zhang F, Zhao Y, Wang Z, Zhou G. Research on 3D-Print Design Method of Spatial Node Topology Optimization Based on Improved Material Interpolation. Mater 2022, Vol 15, Page 3874 2022;15:3874. 10.3390/MA15113874.
[59] Saremi S, Mirjalili S, Lewis A. Grasshopper Optimisation Algorithm: Theory and application. Adv Eng Softw 2017. https://doi.org/10.1016/j.advengsoft.2017.01.004.
[60] Goldberg DE. Genetic algorithms in Search, Optimization and Machine Learning. 1989.
[61] Chen X, Shen SZ. Complete load-deflection response and initial imperfection analysis of single-layer lattice dome. Int J Sp Struct 1993. https://doi.org/10.1177/026635119300800405.
[62] Fan F, Cao Z, Shen S. Elasto-plastic stability of single-layer reticulated shells. Thin-Walled Struct 2010. https://doi.org/10.1016/j.tws.2010.04.004.
[63] Cai J, Xu Y, Feng J, Zhang J. Nonlinear stability of a single-layer hybrid grid shell. J Civ Eng Manag 2012. https://doi.org/10.3846/13923730.2012.723325.
[64] Cai J, Gu L, Xu Y, Feng J, Zhang J. Nonlinear stability analysis of hybrid grid shells. Int J Struct Stab Dyn 2013. https://doi.org/10.1142/S0219455413500065.
[65] Guo J. Research on distribution and magnitude of initial geometrical imperfection affecting stability of suspen-dome. Adv Steel Constr 2011. 10.18057/ijasc.2011.7.4.3.
[66] Bruno L, Sassone M, Venuti F. Effects of the Equivalent Geometric Nodal Imperfections on the stability of single layer grid shells. Eng Struct 2016. https://doi.org/10.1016/j.engstruct.2016.01.017.
[67] Malek S, Wierzbicki T, Ochsendorf J. Buckling of spherical cap gridshells: A numerical and analytical study revisiting the concept of the equivalent continuum. Eng Struct 2014. https://doi.org/10.1016/j.engstruct.2014.05.049.
[68] Mesnil R, Douthe C, Baverel O, Léger B. Linear buckling of quadrangular and kagome gridshells: A comparative assessment. Eng Struct 2017. https://doi.org/10.1016/j.engstruct.2016.11.039.
[69] Batikha M, Mouna Y. Seismic performance of reinforced concrete frame strengthened with an imperfect steel plate shear wall. Int J Struct Eng 2020;10:380. https://doi.org/10.1504/IJSTRUCTE.2020.10030997.
[70] Bulenda T, Knippers J. Stability of grid shells. Comput Struct 2001. https://doi.org/10.1016/S0045-7949(01)00011-6.